2-dimensional imaging of physical information of materials by using pulsed neutron transmission analysis

Y Kiyanagi[1], T Kamiyama[1], H Sato[2], N Ayukawa[1], K Kino[1], F Grazzi[3], and A Scherillo[4]

[1]Hokkaido University, Sapporo, Hokkaido 060-8628, Japan
[2]J-PARC Center, JAEA, Tokai, Ibaraki 319-1195, Japan
[3]CNR-Istituto dei Sistemi Complessi section of Sesto Fiorentin, Florence, Italy
[4]ISIS facility, RAL, Chilton, Didcot, Oxfordshire, Ox11-0QX, UK
E-mail: kiyanagi@qe.eng.hokudai.ac.jp

Abstract. Pulsed neutron transmission gives wavelength dependent neutron intensity reflecting crystallographic structure of materials, dynamics and magnetic field. Therefore, we can obtain a 2-dimensional spatial-dependent image of physical information of materials and fields by analyzing the transmission data observed with a 2-dimensional position sensitive detector. For coherent scatterers, we can get information on preferred orientation (anisotropy), crystallite size and lattice spacing. For such analysis a data analysis code is necessary, and RITS code has been developed. To expand applicable area, further improvement is required. As an application of the crystallographic imaging, investigation on cultural heritages is one of most useful fields. Therefore, we have improved the RITS code and expanded applicable crystal structures, and measured Japanese swords as cultural heritage samples. The crystallite size change from edge to back was observed and difference among three swords was found..

1. Introduction

Spectroscopic imaging using a pulsed neutron source can give information on microstructure of materials, magnetic field and other physical values over a wide area [1-14]. This method uses wavelength dependent transmission through an object. Typical feature of transmission spectrum of a coherent scatterer is Bragg edges appeared at long wavelength region, which corresponds to Bragg scattering at 90 degrees of each crystal plane. To deduce crystallographic information from the transmission spectrum a data analysis code, RITS' was developed[14], and with the aid of this code crystallite size, preferred orientation and also lattice spacing are obtained. However, crystal structures dealt with were limited and multi-phase materials could not be analyzed. Therefore, improvement of the code is required.

As an application of this method imaging of the crystallographic information of cultural heritage is very interesting and useful since it is usually difficult to investigate the cultural heritages in a destructive way. The spectroscopic imaging with neutrons is non-destructive and gives information inside of the cultural heritage. Therefore, it will become possible to obtain information that has not been observed so far.

---

[1] Yoshiaki Kiyanagi

Here, we present recent improvement of the RITS code and the imaging of a Japanese sword as one example of the cultural heritages.

2. Upgrade of the Rietveld-based Bragg edge transmission data analysis code "RITS"

2.1. Issues to be improved

Fig. 1 shows crystalline structural information included in a Bragg edge neutron transmission spectrum obtained by each pixel of a neutron imaging detector. The Rietveld-based Bragg edge transmission data analysis code for pulsed neutron spectroscopic imaging, RITS [14-16], was successfully developed for quantitative evaluation and visualization of various crystalline structural information such as crystallographic texture (preferred orientation) [14,15], microstructure (crystallite size) [14,15] and crystal lattice strain [16,17]. However, the RITS code was not applicable for all crystal structures of 230 types of the space group, a material composed of multi elements and a material composed of multi crystalline phases. Therefore, we have upgraded some functions of the RITS code for solving these issues.

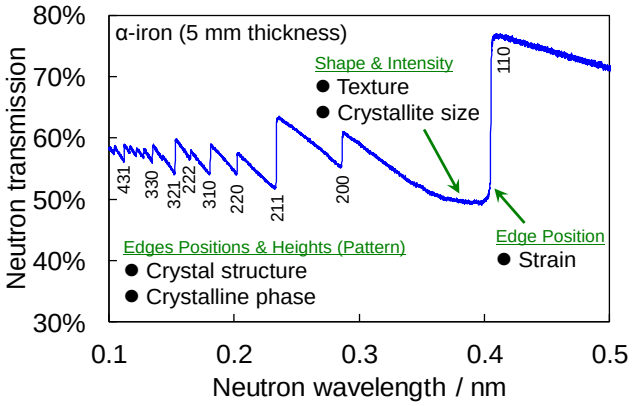

Figure 1. Bragg edge transmission spectrum of a rolled α-Fe plate and including crystalline structural information.

2.2. Consideration on all crystal structures of 230 space groups with multi elements

The neutron transmission spectrum as a function of neutron wavelength $Tr(\lambda)$ is calculated by the Beer-Lambert-Bouguer law,

$$Tr(\lambda) = \exp\left(-\sum_{p} \sigma_{\mathrm{tot},p}(\lambda)\rho_p t_p \right), \tag{1}$$

where $\sigma_{\mathrm{tot},p}(\lambda)$ is the microscopic total cross section, ρ_p is the atomic number density, and t_p is the effective thickness of each crystalline phase p. Furthermore, $\sigma_{\mathrm{tot}}(\lambda)$ consists of elastic coherent scattering, elastic incoherent scattering, inelastic coherent scattering, inelastic incoherent scattering and absorption components, as follows:

$$\sigma_{\mathrm{tot}}(\lambda) = \sigma_{\mathrm{coh}}^{\mathrm{ela}}(\lambda) + \sigma_{\mathrm{incoh}}^{\mathrm{ela}}(\lambda) + \sigma_{\mathrm{coh}}^{\mathrm{inela}}(\lambda) + \sigma_{\mathrm{incoh}}^{\mathrm{inela}}(\lambda) + \sigma_{\mathrm{abs}}(\lambda). \tag{2}$$

In the RITS code, the elastic coherent scattering cross section is calculated by the kinematical diffraction theory [18] combined with the Jorgensen type edge profile function $R_{hkl}(\lambda\text{-}2d_{hkl})$ [19], the March-Dollase preferred orientation function $P_{hkl}(\lambda,2d_{hkl})$ [20] and the Sabine primary extinction function $E_{hkl}(\lambda,2d_{hkl},F_{hkl})$ [21], as follows:

$$\sigma_{\mathrm{coh}}^{\mathrm{ela}}(\lambda) = \frac{\lambda^2}{2V_0}\sum_{hkl}\left|F_{hkl}\right|^2 d_{hkl}R_{hkl}(\lambda - 2d_{hkl})P_{hkl}(\lambda,2d_{hkl})E_{hkl}(\lambda,2d_{hkl},F_{hkl}), \tag{3}$$

where V_0 is the unit cell volume of the crystal lattice, F_{hkl} is the crystal structure factor, and d_{hkl} is the crystal lattice plane spacing. The crystal structure factor F_{hkl} is calculated by

$$F_{hkl} = w_{hkl} \sum_n o_n b_n \exp\left[2\pi \mathrm{i}\left(hx_n + ky_n + lz_n\right)\right] \exp\left(-\frac{B_{\mathrm{iso},n}}{4d_{hkl}^2}\right). \quad (4)$$

Here, w_{hkl} is the multiplicity. o_n is the site occupancy, b_n is the coherent scattering length, (x_n,y_n,z_n) is the fractional coordinates, and $B_{\mathrm{iso},n}$ in the Debye-Waller factor is the isotropic atomic displacement parameter, of n-th site atom in the crystal lattice.

In the improved RITS code, a new subroutine was implemented for automatic calculation of the crystal structure factor of all the crystal structures. This component reads the space symmetry parameters, the rotation matrices $\boldsymbol{R}$ and the translation vector $\boldsymbol{T}$, from the database containing the information of coordinates of equivalent positions of 230 space groups, and can automatically give the all atomic coordinates in the crystal lattice by using only n-th site fractional coordinates (x_n,y_n,z_n) information and the equivalent coordinates information. Then, s-th equivalent position of n-th site general position is given by Ref. [22],

$$\begin{pmatrix} x_{ns} \\ y_{ns} \\ z_{ns} \end{pmatrix} = \begin{pmatrix} R_{11s} & R_{12s} & R_{13s} \\ R_{21s} & R_{22s} & R_{23s} \\ R_{31s} & R_{32s} & R_{33s} \end{pmatrix} \begin{pmatrix} x_n \\ y_n \\ z_n \end{pmatrix} + \begin{pmatrix} T_{1s} \\ T_{2s} \\ T_{3s} \end{pmatrix} = \begin{pmatrix} R_{11s}x_n + R_{12s}y_n + R_{13s}z_n + T_{1s} \\ R_{21s}x_n + R_{22s}y_n + R_{23s}z_n + T_{2s} \\ R_{31s}x_n + R_{32s}y_n + R_{33s}z_n + T_{3s} \end{pmatrix}. \quad (5)$$

Owing to this new component, the RITS code can automatically calculate the crystal structure factor of 230 space groups and also a crystal structure composed of multi-elements at the same time. Fig. 2 shows simulation calculation results of microscopic total cross sections of magnesium having the HCP (hexagonal close packed) structure (space group number 194) and hydrogen storage alloy $Ti_{0.45}Cr_{0.25}Mo_{0.30}$ (space group number 229), calculated by the improved RITS code. The Bragg edge pattern of the HCP structure and the effects of negative scattering length of Ti (weak Bragg diffraction and inelastic scattering emphasized) are successfully produced.

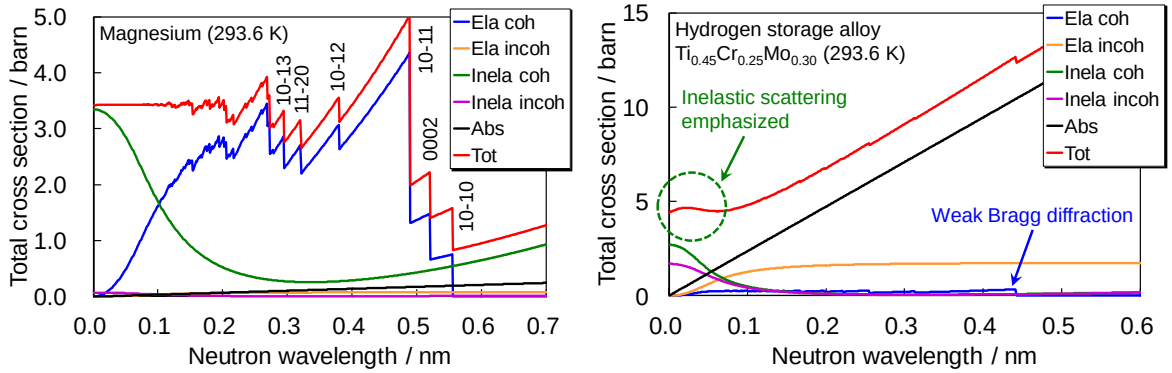

Figure 2. Simulation calculation results of microscopic total cross section of magnesium (left) and hydrogen storage alloy $Ti_{0.45}Cr_{0.25}Mo_{0.30}$ (right) by the improved RITS code.

2.3. Quantitative evaluation of a material with multi crystalline phases

For quantitative crystalline phase imaging, it is necessary to evaluate the quantity of each phase. In the improved RITS code, the projected atomic number density (atomic number density × effective thickness) $\rho_p \times t_p$ of each phase can be evaluated. The experimental pulsed neutron transmission data were measured at BL20 at Materials and Life Science Experimental Facility (MLF) at Japan Proton Accelerator Research Complex (J-PARC) in Japan [23]. The sample was a welded plate of JIS-SS400 (alpha-iron, the BCC (body centered cubic) structure) and JIS-SUS304 (austenite stainless steel Fe 9%Ni 19%Cr, the FCC (face centered cubic) structure) of 6 mm thickness. The neutron imaging detector was the ^{6}Li-glass scintillator pixel-type detector (64 pixels type) [3, 24].

Fig. 3 indicates that the profile fitting to the transmission data at an area of mixed two-phases. It is clearly shown that mixed analysis of BCC and FCC phases precisely reproduces the experimental transmission data, which proves the usefulness of the improved RITS code.

Thus, the improved RITS code is applicable for all crystal structures of 230 types of space group, a material composed of multi elements and a material composed of multi crystalline phases.

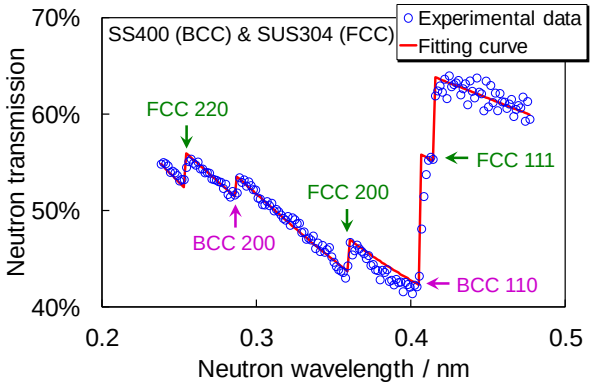

Figure 3. Fitting to a SS400/SUS304 mixed area transmission spectrum by using the improved RITS code.

3. Imaging of a Japanese sword

We analyzed the crystallite information of Japanese swords as one of historical heritages. Japanese swords have a long history. Therefore, differences in the crystallite information depending on production ages and places in Japan are expected. Moreover, the crystallite information is expected to vary depending on the position on a Japanese sword.

We studied three Japanese swords. Their production ages and places are as follows. Sample 1: The mid of 16th century, Bishu (Okayama prefecture). Sample 2: The late of 17th century, Bizen (Okayama prefecture). Sample 3: The mid of 16th century, Sohshu (Kanagawa prefecture). Two types of measurements were performed. One is the measurement at the Hokkaido University Neutron Source (HUNS) to study differences of the crystalline information among the three samples. The other is the measurement at the ISIS facility in the Rutherford Appleton Laboratory to study differences of the crystallite information depending on the position of the sample 1. The two-dimensional neutron detector, GEM (Gas Electron Multiplier) was used for these two measurements. This detector has a sensitive area of 10cm×10cm and a position resolution of 0.8 mm.

The photo of the measurement at HUNS is shown in Fig. 4. The three samples were set in parallel. The neutron detector is behind the samples. We analyzed the data in the rectangular areas, which correspond to the back (i.e. opposite sides of the edge) of the samples. The cross sections converted from the transmission data are in Fig. 5. The Bragg edge around 0.4 nm is the {110} diffraction for α iron. The cross sections are different between the {110} diffraction and the next diffraction ({200}) around 0.28 nm. The cross section of the sample 3 is smaller than those of the sample 1 and 2. This implies that the crystalline size of the sample 3 is large comparing to those of other samples. Moreover, the dependences of the cross sections of the samples 2 and 3 on the neutron wavelength are close to a function of square of the wavelength. This implies that the crystal orientation is more isotropic. On the other hand, the dependence of the sample 1 is largely different from those of other samples and suggests the anisotropy. We analyzed the time-of-flight spectra by the RITS code and obtained the data of the crystalline size and crystal orientation anisotropy. The crystalline sizes of the sample 1 (2.99μm) and 2 (2.93μm) are almost the same. On the other hand, the crystal size of the sample 3 (3.70μm) is larger than those of other samples. This result is consistent with the qualitative analysis mentioned above. Japanese swords are made of wrought steel. The crystalline size is expected to be smaller for well-wrought steel. Therefore, this result could be due to the difference of the production processes depending on the place in Japan. About the index of the crystal orientation anisotropy, 1 is for the complete isotopic orientation and the index becomes smaller or bigger than 1 if the crystal orientation becomes anisotropic. The sample 2 (0.90) is relatively isotopic comparing to other two samples (sample 1: 1.99, sample 3: 1.34) and this could be due to the difference of the production age.

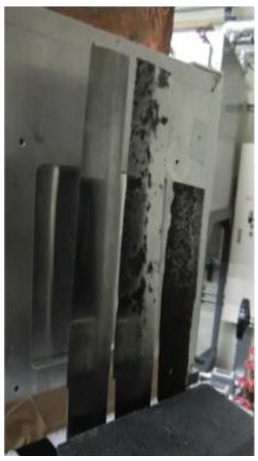

Figure 4. Photo of the measurement at HUNS.

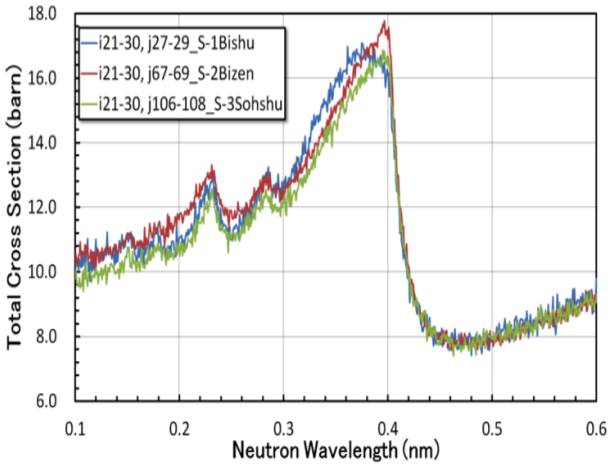

Figure 5. Total neutron cross sections of three swords.

Figure 7 and 8 are two-dimensional plots of the crystalline size and orientation anisotropy obtained by the ISIS experiments for the sample 1. The crystal size increases from the edge to the back. This could originate from the unique production process of Japanese swords. The steel called "Kawagane" wraps the core steel called "Shingane". The Shingane is the soft steel, of which crystal size is large. The Kawagane is the hard steel, of which crystal size is small because it is well-wrought steel. The Shingane makes Japanese swords hard to break and the Kawagane cut well. The ratio of the Kawagane to the Shingane is large at the edge comparing to the back. Therefore, the crystalline size was small around the edge as shown in Fig. 7. On the other hand, crystal orientation anisotropy varies from the core called "Nakago" to the tip and becomes strong towards the tip side. This may be due to making process of these areas.

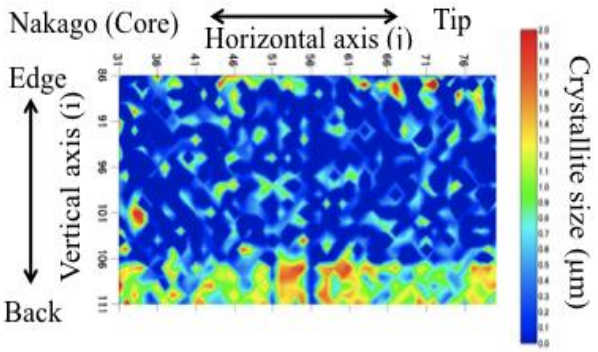

Figure 6. Crystallite size distribution

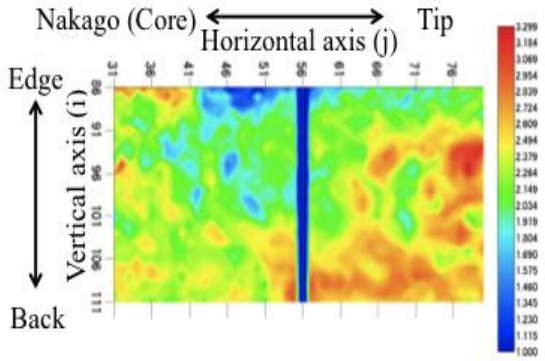

Figure 7. Crystal orientation distribution.

As mentioned above, we showed that the pulsed neutron imaging was an effective method for studying characteristics of the swords depending on the production age and place, and crystal information depending on the position on a Japanese sword. Systematic study is expected by increasing the number of samples. Moreover, cultural and historical insight will be obtained for other historical heritages also.

4. Summary

The pulsed neutron transmission imaging has expanded its applicability owing to the improved data analysis code. Furthermore, it has been indicated that the method is useful for investigating the cultural heritages. Here, we only described the imaging of the crystallographic information, and the imaging of hydrogen dynamical state in materials such as hydrogen storage materials will be possible.

Therefore, it should be considered to apply this method to various fields not only in material science and but also engineering development.

References

[1] Santisteban J R, Edwards L, Steuwer A and Withers P J, 2001 *J. Appl. Crystallogr.* **34**, 289
[2] Santisteban J R, Edwards L, Fizpatrick M E, Steuwer A, Withers P J, 2002 *Appl. Phys. A* **74** S1433
[3] Mizukami K, Sato S, Sagehashi H, Ohnuma S, Ooi M, Iwasa H, Hiraga F, Kamiyama T and Kiyanagi Y, 2004 *Nucl. Instr. and Meth. Phys. Res.* **A529** 310
[4] Kiyanagi Y, Kamiyama T, Iwasa H and F. Hiraga F, 2004 *Key Engineering Materials* **270** 1371
[5] Kiyanagi Y, Sakamoto N, Iwasa H, Kamiyama T, Hiraga F, Sato S, Sagehashi H, Ino T, Furusaka M, Suzuki J, Gorin A, Manuilov I, Ryazantsev A, Kuroda K, Sakai K, Tokanai F, Miyasaka H, Adachi T, Oku T, Ikeda K, Suzuki S, Morimoto K, and Shimizu H M 2005 *IEEE Tran.Nuclear Science* **52** 371
[6] Kiyanagi Y, Mizukami K, Kamiyama T, Hiraga F and Iwasa H 2005 *Nucl. Instr. and Meth., Phys. Res.* **A542** 316
[7] Kiyanagi Y, Kamiyama T, Nagata T and Hiraga F 2006 *Key Eng. Mat.* **321-323** 1663
[8] Iwase K, Sakuma K, Kamiyama T and Kiyanagi Y, 2009 *Nucl. Instr. Meth. Phys. Res.* **A605** 1
[9] Takada O, Kamiyama T and Kiyanagi Y 2010 *J. Nucl. Mat.* **398** 1
[10] Kiyanagi Y, Kamiyama T, Sato H, Shinohara T, Kai T, Aizawa K, Arai M, Harada M, Sakai K, Oikawa K, Ohi M, Maekawa F, Sakai T, Matsubayashi M, Segawa M and Kureta M 2011 *Nucl. Instr. Meth. Phys. Res.* **A 651** 16
[11] Shinohara T, Sakai K, Ohi M, Kai T, Harada M, Oikawa K, Maekawa F, Suzuki J, Oku T, Takata S, Aizawa K, Arai M and Kiyanagi Y 2011 2011 *Nucl. Instr. Meth, Phys. Res. **A 651*** 121
[12] Kai T, Segawa M, Ooi M, Hashimoto E, Shinohara T, Harada M, Maekawa F, Oikawa K, Sakai T, Matsubayashi M and Kureta M 2011 *Nucl. Instr. and Meth, Phys. Res.* **A 651** 126
[13] Strobl M, Kardjilov N, Hilger A, Penumadu D and Manke I 2011 *Nucl. Instr. Meth. Phys. Res.* **A 651** 57
[14] Sato H, Kamiyama T and Kiyanagi Y 2011 *Mater. Trans.* **52** 1294
[15] Sato H, Kamiyama T, Iwase K, Ishigaki T and Kiyanagi Y 2011 *Nucl. Instr. Meth. Phys. Res.* **A 651** 216
[16] Kiyanagi Y, Sato H, Kamiyama T and Shinohara T 2012 *J. Phys. Conf. Ser.* **340** 012010
[17] Iwase K, Sato H, Harjo S, Kamiyama T, Ito T, Takata S, Aizawa K and Kiyanagi Y 2012 *J. Appl. Crystallogr.* **45** 113
[18] Fermi E, Sturm W J and Sachs R G 1947 *Phys. Rev.* **71** 589
[19] Vogel S 2000 *Ph. D. Thesis* Christian Albrechts Universität
[20] Larson A C and Von Dreele R B 2004 *LAUR 86-748* Los Alamos National Laboratory
[21] Sabine T M, Von Dreele R B and Jørgensen J -E 1988 *Acta Crystallogr. Sec. A* **44** 374
[22] Izumi F and Momma K 2007 *Solid State Phenom.* **130** 15
[23] Iwase K, Sato H, Mori K, Kamiyama T, Ishigaki T and Kiyanagi Y 2011 *Metall. Mater. Trans. A* **42** 2296
[24] Sato H, Takada O, Satoh S, Kamiyama T and Kiyanagi Y 2010 *Nucl. Instr. Meth. Phys. Res.***A 623** 597

Acknowledgments
This work was supported by KAKENHI (23226018) and for the use of the GEM detector also by the support program of accelerator science by KEK.